A Comparative Analysis of 2D and 3D Cell Culture Techniques for Understanding Endometrial Cancer

Nery A. Matias Calmo, Christian A. Merino

Abstract

Endometrial cancer is a prevalent gynecological malignancy with significant health risks to millions of people around the world. Developing an *in vitro* model of the endometrium is crucial for gaining a deeper understanding of the disease and advancing specialized treatments. In this study, we used both 2D and 3D cell culture to model the endometrium using GMMe and L929 cells. Five different treatments were administered to each cell type, including estradiol, progesterone, and a combination of both, to mimic the follicular and luteal phases of the menstrual cycle. The effects of the treatments were analyzed using various assays, including Presto Blue, ELISA, and LDH assays. The cells were then seeded onto chitosan scaffolds to examine their growth and organization in a three-dimensional environment. Statistical analysis, including ANOVA tests, were preformed to evaluate the significance of the data. Results of this study will aid in the development of a functional endometrial model, allowing for a better understanding of the effects caused by endometrial cancer and discover possible treatments to the disease. By replicating the endometrial environment, models of endometrial cancer *in vitro* can allow for the identification of the causes of the disease as well as create effective therapies to slow disease progression. It will also allow for the study of the advantages and limitations of 2D and 3D cell culture techniques to create physiologically relevant models in investigating complex cellular behaviors and interactions. Ultimately, this research as the potential to deepen understanding of the endometrium and have applications to creating experimental treatments for endometrial cancer.

Introduction

Cancer within the endometrium is extremely prevalent in the United States, as estimates indicated that there would be 61,880 new cases and 12,160 deaths in 2019 [1]. It is the most diagnosed gynecologic cancer for women in the United States. Since it is one of the leading health risks for women in the country, it is essential to work towards developing an *in vivo* model of the endometrium to gain a better understanding of the disease. Creating an intuitive model for both researchers and patients alike to interact with will lead to the development of more specialized treatments along with an increased ability for patients to make informed health decisions concerning traditional and experimental treatments.

The endometrium is the tissue lining the uterus, and the cells within the endometrium undergo many changes in shape and behavior as they progress through the menstrual cycle. [2] The tissue of the endometrium plays an essential part in reproduction as the physiological changes within the cells allow for the body to be prepared for pregnancy or menstruation. Endometrial tissue is made up of endometrial stromal cells, and they are classified as fibroblasts. The endometrium also contains epithelial cells which function in tandem in the fibroblasts. Learning more about the ways in which endometrial cancers disrupt the many processes of the endometrium will lead to a higher likelihood of survival and a restoration of function.

Figure 1: Uterus Histology

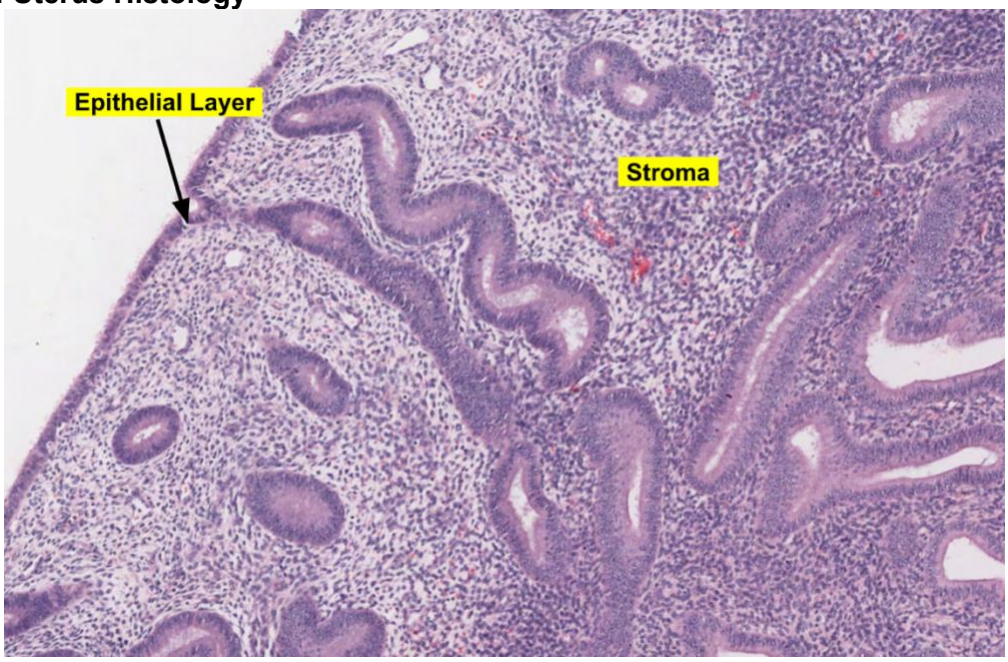

Yong Loo Lin School of Medicine - National University of Singapore, Uterus-Normal Histology, https://medicine.nus.edu.sg/pathweb/normal-histology/uterus/

Epithelial cells in the endometrium primarily compose the lining and are important for ensuring the proper endometrial receptivity. These cells protect the endometrium along with providing an ideal location for life to be started and maintained[3]. The morphology of the epithelial cells found in the endometrium have been found to be mostly cuboidal. The endometrial stromal cells or fibroblasts, function as agents for proliferation of the tissue. They also have a large role in remodeling the lining of the uterus following the completion of the menstrual cycle. Their morphology in the endometrium has been observed to be more elongated compared the morphology of the epithelial cells, taking on a spindle like shape.

Figure 2: Hormones in the Menstrual Cycle

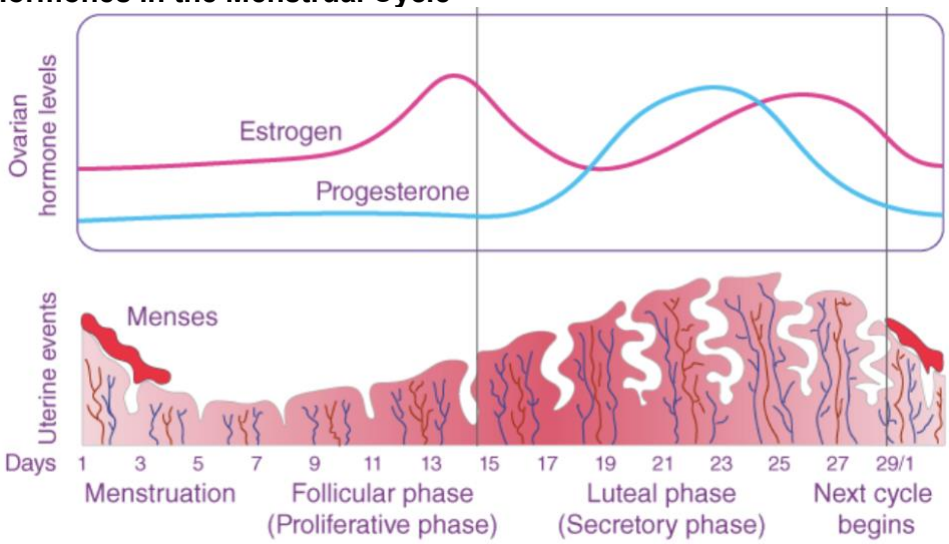

Admin (2022) Menstrual cycle- phases of menstrual cycle and role of hormones, BYJUS, https://byjus.com/biology/menstrual-cycle/

The endometrium undergoes a hormone cycle consisting of three phases: the menses phase, follicular (proliferative) phase, and the luteal (secretory) phase. In the menses phase, the outer lining of the uterus is shed when pregnancy hasn't occurred and occurs monthly. The follicular phase is characterized by an upregulation in estrogen levels and cell proliferation to prepare for ovulation, while the secretory phase is instead characterized by a decrease in estrogen and an increase in progesterone levels[4]. It is possible for women to develop hyperplasia of the endometrium due to improper regulation of hormones and the proliferative phase. Hyperplasia within the endometrium can be an early sign of cancer development, thus emphasizing the need for a functional endometrial model to be created. In healthy women, the proliferative phase causes the tissue of the uterus lining to thicken.[5] On a cellular level, the cells that make up the endometrium are actively multiplying. During the secretory phase, the tissue of the endometrium undergoes changes in morphology to prepare the body for a possible pregnancy. The secretory phase also involves the cells releasing a secretion filled with glycogen.

2D cell culture and microscopy refers to the growth of cells in a flat, two-dimensional surface like a Petri dish or a culture flask. In this type of cell culture, cells are grown and adhered in one layer. Using 2D cell culture and microscopy, we can observe various aspects of cell behavior and function, including cell morphology, cell proliferation, cell migration, and cell differentiation. For example, we can use microscopy to visualize the overall morphology of the cells and determine the size, shape, and density. We can then use stains such as the Dapi and Actin stain to visualize specific cellular components or proteins and observe their location and expression levels within the cells. In addition to looking at individual cells, microscopy allows the study of cell-to-cell interactions in the ECM such as the formation of junctions and the communication between cells. There are many pros and cons that comes with 2D cell culture and microscopy. For example, some of the pros of this type of cell culture is the simplicity that 2D cell culture provides as it is easy to set up and maintain and it can also be performed using simple and inexpensive equipment. Also, this method allows for easy use though screening assays to test large numbers of compounds to study the effects on the surrounding cells. Some of the cons to using 2d cell culture and microscopy is that there is a lack of physiological relevance since cells grown in the 2D may behave differently than cells *in vivo*, as they don't have the complex three-dimensional structure and extracellular matrix that cells encounter in their natural environment. Also overcrowding is a possibility which can lead to changes in gene expression and cell behavior if the flask/dish isn't maintained or monitored properly.

In 3D cell culture, cells are grown in a three-dimensional structure that mimics the *in vivo* environment where they are grown in a matrix or scaffold that provides physical support and allows for the formation of cell-cell and cell-matrix interactions. Using this method, we can observe and learn many things about cell behavior and function that are otherwise more difficult to observe in 2D. For example, cell migration can be analyzed to provide insights into how cells move and migrate through tissues, since cells may migrate in different directions and exhibit different migration speeds depending on their location within the matrix. It also allows for the study of tissue development and the formation of organ-like structures which help create models to study disease progression or mimic conditions for the formulations of treatments to these diseases. Cells grown in a 3D cell culture can self-organize and differentiate into tissue-like structure that more closely resemble *in vivo* tissues. There are many pros and cons to 3D cell culture. For example, one pro is that 3D cell culture allows for the mimic of the *in vivo* environment and provides a more physiologically relevant environment than in 3D cell culture which allows for a better portrayal of the *in vivo* tissue architecture, and interactions between cells and the matrix. Also, it allows for reduces animal usage since 3D cell culture can reduce the number of animal experiments required in drug testing, as it provides a more reliable alternative to animal models. One disadvantage of 3D cell culture is its technical complexity

where 3D cell culture techniques are often more complex and require specific equipment and expertise, which can make them more challenging to implement.

Scaffolds and biomaterials are two related concepts in 3D cell culture that play a critical role in the growth and organization of cells. A scaffold is a three-dimensional structure used to support the growth and organization of cells, providing a physical framework for cells to adhere to and interact with. Scaffold can be made from a variety of materials, including nature and synthetic ones. Scaffolds are designed to have specific physical and chemical properties such as porosity and stiffness which can be tailored to the specific tissue or application being studied. Scaffolds are often made from biomaterials that are biocompatible and able to interact with cells in a way that promotes tissue growth and regeneration. The scaffold material must be able to support cell attachment and growth, while also allowing for nutrient and waste exchange. Biomaterials used need to be non-toxic, non-immunogenic, and biodegradable, meaning they can be broken down and removed from the body as new tissue forms.[6]

In this study, we used two ways of cell culture to model the endometrium; 2D cell culture and 3D cell culture. We used two cell types, GMMe and L929 cells; and conducted five different treatments on each cell type: untreated, 10nM of estradiol (mimics the follicular phase), 10 uM progesterone, and both 10nM estradiol and 10 uM progesterone (mimics the luteal phase). After treatment, we fixed and stained the cells using a Dapi and actin stain and analyzed the effects by conducting a Presto Blue assay and ELISA assay. The cells were then seeded onto chitosan scaffolds and a Presto Blue assay and an LDH assay were conducted. An ANOVA test was conducted on all the data to see if the data acquired was statistically significant and if it aligned with the rest of the data taken. It is hypothesized that the treatment with 10 uM of estradiol will have the most cell proliferation in the GMMe cell type by mimicking the follicular phase, while the treatment of estradiol and progesterone will have the most cell proliferation in the L929 cell type by mimicking the luteal phase. Once we can model the endometrium, then applications of the data will be suitable for creating disease models of endometrial cancer *in vitro* to find suitable treatments that can slow the progression of the disease.

Materials and Methods

Materials

Fetal bovine serum (FBS), antibiotic-antimycotic, Dulbecco's phosphate-buffered saline (DPBS), trypsin 0.25%, dimethylsulfoxide (DMSO), 4% paraformaldehyde, Dulbecco's Modified Eagle Medium Nutrient Mixture F-12 (DMEM-F12), DMEM-F12 with no phenol red, MEM-F12, estradiol, 70% ethanol, and fibronectin were purchased from Thermo Fisher Scientific. Progesterone, chitosan with medium molecular weight, glacial acetic acid, sodium hydroxide 10N, and lactate dehydrogenase kit (LDH) containing NAD+, diaphorase, sodium lactate and iodo-tetrazolium chloride (INT) were purchased from Sigma-Aldrich. The cell mask actin statin, 4',6-diamidino-2-phenylindole (DAPI) stain, insulin-like growth factor 1 enzyme-linked immunosorbent assay kit (IGF-1 ELISA), and presto blue solution were purchased from Invitrogen. The L-929 cells and GMMe cells were purchased from ATCC Global Bioresource Center.

Cell Culture

To begin the cell culturing process, the DMEM media + 10% FBS + 1% anti-anti was warmed in a media bath at 37 degrees Celsius. The warm conditions for the media are meant to facilitate cell growth. Once a sufficient time had elapsed, 10 mL of the warm media was added to the cell flask. The cells used throughout the experiment were kept in a freezer with temperature of -80 degrees Celsius in order to preserve the cells to eventually be cultured. After the cell vial was retrieved from the freezer, they needed to be thawed by loosening the cap and placing them in a warm water bath for a short period of time. Once thawed, 1 mL of cells were added to the cell flask containing the media. The flask was then placed in an incubator at 5% CO2 and 37 degrees Celsius. The conditions within the incubator are optimal for cell growth as

the presence of carbon dioxide preserves a pH neutral environment for the cells, which along with room temperature will allow the cells to grow.

After the cells were given time to grow, they were examined under the microscope in order to determine the percent of cell coverage and the cell shape. PBS was added to the cell flask to reduce the concentration of unhealthy cells. 2mL of trypsin was then added to the cell flask, and after a brief incubation period the reagent was able to lift the cells from the bottom of the flask. To remove the rest of the cells adhered to the bottom of the flask, media was added and then aspirated several times. The final solution was then added to a 15mL tube in order to be counted by the hemocytometer. Using calculations derived from the hemocytometer, media was added back to the cell pellet and placed into a different container to be frozen. 1mL of the new cell solution was added to the flask along with 9mL of fresh media to be placed into the incubator. Finally, a solution of 5% DMSO in media was created and 1mL was transferred into two separate vials. The vials were then placed into the "Mr. Frosty" device.

Microscopy

The wells used for the samples were rinsed several times with PBS. 250µL of 4% paraformaldehyde was added to the plate to eventually enter incubation. The wells were then rinsed again multiple times with PBS. In two wells, 250µL of cell mask actin stain was added and kept under foil to incubate for 15 minutes. The wells were rinsed with PBS afterwards. Next, 250µL of DAPI stain was added to the two wells and incubated under foil for 5 minutes. Once again, the wells were rinsed with PBS. Upon completion of this procedure, images were taken of each sample in brightfield, green filter (for actin), and blue filter (for nuclei).

2D Biochemical Study

Samples were diluted and the incubated in antibody coated wells for 3 hours before the biochemical study procedure had begun. There were 4 different treatments created for both L929 cells and GMMe cells. Each cell type had an untreated case, a case treated with 10nM estradiol, a case treated with 10 µM progesterone, and a case treated with both 10nM estradiol and 10µM progesterone. Each hormone treatment was given over a 48-hour period, and in total there were 8 different wells with these samples. 200µL of wash buffer was then used to remove excess antigen from each well in the plate. 100µL of biotin conjugate was then added to each well in order to incubate for 50 minutes. The presto blue reagent was then added to wells, which helps to determine the overall viability of the cells after they are treated with their selected hormones. 100µL of streptavidin-HRP was then added to the wells and allowed to incubate for 40 minutes. Afterwards, 100µL of TMB substrate was added to each well and allowed to incubate for 30 minutes. While the wells were incubating, the presto blue wells were retrieved from the incubator. 200µL of each sample were added to an empty 96 plate well, and the plate was read at 560 nm and 590 nm. After the TMB substrate concludes incubation in the other wells, 50µL of stop solution is added to each well and the plate absorbance is read at 450 nm.

Scaffolds and Biomaterials

In this study, chitosan, a natural polymer derived from crustacean and insect exoskeletons, was chosen as the material for scaffold preparation. Chitosan shared similarities with glycosaminoglycans (GAGs), which are abundant in the extracellular matrix, making it suitable for mimicking the natural cellular environment. Since chitosan is insoluble at neutral pH, the material is dissolved in 2M acetic acid at a concentration of 2%. The solution was then poured into a 24 well plate mold to give the scaffold its desired shape. The sponge-like and porous structure within the scaffold was created using a process called lyophilization (freeze drying). During lyophilization, the solution is rapidly frozen, leading to the formation of ice crystals throughout the solution. The frozen samples are then placed under a vacuum, allowing the ice to sublime. This results in pores being formed where the ice crystals were previously

located, the size and morphology of the scaffold can be controlled by adjusting the freezing temperatures and time. After lyophilization. The chitosan scaffold contains residual protonating ions from the acetic acid, which can destabilize the chitosan in cell culture conditions. To neutralize these ions and stabilize the scaffold, a basic solution of NaOH was used to rinse the scaffolds. To ensure a sterile environment, the chitosan scaffolds are then sterile by treating the scaffolds with 70% ethanol which eliminates microorganisms and prepares them for cell seeding and storage.[7]

3D Biochemical Study

Once the scaffolds were seeded with cells and cultured for a week, 10% fetal bovine serum (FBS) was added for 48 hours, followed by a change of 5% FBS media for 72 hours. The decrease in serum concentration was intended to potentiate the treatments added to the cells. By reducing the concentration, the cells may become more sensitive and responsive to the treatments, allowing them to have a greater impact on controlling cell growth and replication. The hormone treatment with 5% FBS and media was added for 48 hours followed by a biochemical analysis of Lactate Dehydrogenase (LDH) and Presto Blue. A sample was removed to conduct an LDH assay to measure the glycolysis activity of the cells. In the LDH assay, the enzyme, lactate dehydrogenase is studied which catalyzes the conversion of lactate to pyruvate with the reduction of NADH+ to NADH in the final step of glycolysis. Expression of this enzyme is increased during the luteal phase as cells are differentiating and preparing the endometrium for implantation and will aid in identifying the luteal phase in the scaffolds with heightened expression of LDH. Afterwards, the Presto Blue reagent was added to measure cell proliferation in the scaffolds. In the Presto Blue assay, the cell viability is analyzed based on the cells ability to reduce a colorless dye, resazurin, to a fluorescent dye, resorufin. This assay works on the condition that metabolically active cells possess mitochondrial reductase, which converts resazurin to resorufin. Resorufin emits a strong fluorescence signal that can be quantified using a microplate reader. Since proliferation is upregulated more in the follicular phase than in the luteal phase, this assay will allow for the identification of the follicular phase in the scaffolds where increased cellular proliferation is present.[8]

Statistics

After gathering the data in the biochemical study, a statistical analysis was conducted on all the data points to study the statistical relevance of the data sets. An Analysis of Variance (ANOVA) test was conducted to determine whether there is a significant difference between the averages of two or more groups. More specifically, a two-factor ANOVA test was conducted to study the variance between two groups in the study: the cell type and hormone treatments. Data analysis of both the 2D (Presto Blue and ELISA) and 3D (Presto Blue and LDH) data sets were done to analyze which parameter affected the results in the study. The p-values were found which represent the probability of observing the statistic that was calculated, assuming that the null hypothesis is true (which is that there is no significant difference between the groups). A low p-value (one below 0.05) suggest that the observed differences are unlikely due to random chance which means the null hypothesis is rejected and is concluded that there is a significant difference between the two groups being compared. A high p-value (one above 0.05) suggest that there is less evidence against the null hypotheses meaning, the observed results were likely due to chance and that there is no significant difference between the groups.[9]

A Turkey's test or Turkey-Kramer test is a test that is conducted after an ANOVA test to determine the significant differences between the group averages. In this study, only if the p-values for the hormone treatments were considered for this test so if the p-value for the cell type is significant then no post-testing is needed. However, if the p-value for the hormone treatment is less than 0.05 then the differences between the 4 treatments groups is significant and each

was compared for each cell type. To compare them, the differences in the means of each pair and the mean squares from the ANOVA was used to calculate the Turkey value.[10]

Results and Discussion

Figure 3: 2D Microscopy Images

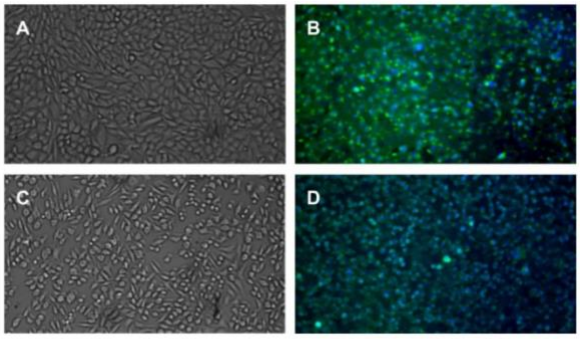

Figure 3: A.) Brightfield microscopy of the GMMe endometrial epithelial cells. B.) Fluorescent overlay microscopy of the GMMe endometrial epithelial cells. C.) Brightfield microscopy of the L929 fibroblasts. D.) Fluorescent overlay microscopy of the L929 fibroblasts

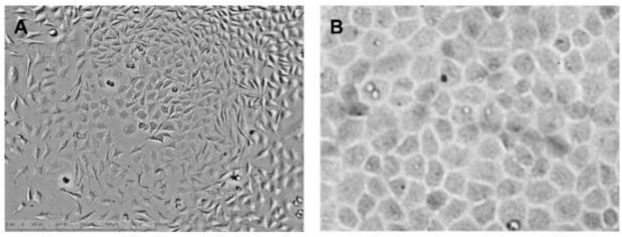

*Figure 4: A.) L929 mouse fibroblasts. Fibroblasts have a spindle-shaped morphology. B.) GMMe mink endometrial epithelial cells. Epithelial cells have a cuboidal morphology. ***CITATIONS*

Actin stains are used to highlight the cytoskeleton found within the cuboidal epithelial cell, while the DAPI stain highlights the nuclei and more specifically the spindles that are present. L929 cells have an elongated spindle-like shape, while the GMMe cells have a rounder shape to them with some clumps being present. The L929 cells are shaped in this way in order to provide support to the cells, and ultimately maintain a level of homeostasis. The shape of GMMe cells are important as they function as lining for the endometrium, and their tendencies to group together can be indicative of behaviors seen in cancerous cells or tissues. The shapes of each of the cell types has significance in their functions. The shapes of each cell also help researchers model different phenomena in the body. The shape and function of L929 cells can be used a model to understand and gauge cell proliferation along with cell differentiation. On the other hand, the morphology and role of GMMe cells can be used a model for tumor behavior and thus a model for cancer as well.

Figure 4: Average Presto Blue Results and ANOVA

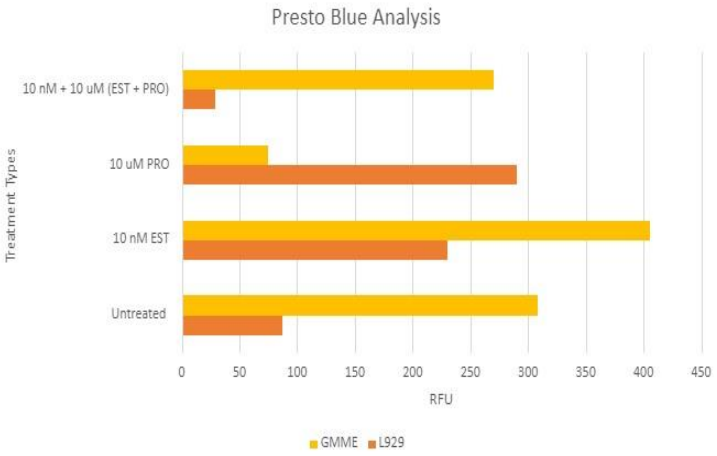

Anova: Two-Factor With Replication

SUMMARY	Untreated	10 nM EST	10 uM PRO	10 nM + 10 u	Total
L929					
Count	4	4	4	4	16
Sum	0.2889	0.2992	0.3416	0.3776	1.3073
Average	0.072225	0.0748	0.0854	0.0944	0.08170625
Variance	0.0003027	0.00041677	0.00030491	0.00021254	0.00033068
GMME					
Count	4	4	4	4	16
Sum	0.3182	0.3129	0.3241	0.3963	1.3515
Average	0.07955	0.078225	0.081025	0.099075	0.08446875
Variance	0.00037055	0.00020796	0.00016044	0.00115956	0.0004566
Total					
Count	8	8	8	8	
Sum	0.6071	0.6121	0.6657	0.7739	
Average	0.0758875	0.0765125	0.0832125	0.0967375	
Variance	0.00030386	0.00027109	0.0002049	0.00059429	

ANOVA

rce of Variat	SS	df	MS	F	P-value	F crit
Sample	6.1051E-05	1	6.1051E-05	0.15577146	0.69656547	4.25967727
Columns	0.00225127	3	0.00075042	1.91469529	0.15415597	3.00878657
Interaction	0.00015171	3	5.0571E-05	0.12903188	0.94191874	3.00878657
Within	0.00940628	24	0.00039193			
Total	0.01187032	31				

Concentrations (w/o Dilution) (pg/mL)	Untreated	10 nM EST	10 uM PRO	10 nM + 10 uM (EST + PRO)
L929	2622.776247	2622.708661	2622.430446	2622.194226
GMME	2622.58399	2622.618766	2622.545276	2622.071522

1 pg = 0.001 ng | Formula | y = 0.0381 x + 100

0.001

Concentrations (w/o Dilution) (ng/mL)	Untreated	10 nM EST	10 uM PRO	10 nM + 10 uM (EST + PRO)
L929	2.622776247	2.622708661	2.622430446	2.622194226
GMME	2.62258399	2.622618766	2.622545276	2.622071522

Dilution Fact. 50

Estimated Concentrations (w/ Dilution) (ng/mL)	Untreated	10 nM EST	10 uM PRO	10 nM + 10 uM (EST + PRO)
L929	131.1388123	131.1354331	131.1215223	131.1097113
GMME	131.1291995	131.1309383	131.1272638	131.1035761

The graph shows averaged results for the Presto Blue assay. It compares L929 and GMMe cell types with treatments of estradiol, progesterone, estradiol + progesterone, along with a negative treatment with none of the hormones present. The ANOVA table depicts possible statistically significant differences between cell type and type of treatment

The presto blue average results showed visible differences between cell types and treatments. The highest level of cell viability can be seen in GMMe upon undergoing the treatment with 10 nM estradiol. On the other hand, the lowest cell viability can be seen in the GMMe cells upon undergoing the treatment with both estradiol and progesterone. The ANOVA results indicate that all the p-values are over 0.05, meaning that there are no statistically significant differences between the treatments and cell types. The presto blue assay essentially measures the number of healthy cells in each of the samples, and this is usually referred to as cell viability. For connective tissue cells, such as GMMe, cell viability is important to keep linings within the body intact. L929 cells, or fibroblasts, are important in forming the connective tissue needed in the body along with maintaining homeostasis through mechanisms of injury repair and remodeling.

Figure 5: Average IGF-1 ELISA Results and ANOVA

Anova: Two-Factor With Replication

SUMMARY	Untreated	10 nM EST	10 uM PRO	10 nM + 10 u	Total
L929					
Count	4	4	4	4	16
Sum	0.2889	0.2992	0.3416	0.3776	1.3073
Average	0.072225	0.0748	0.0854	0.0944	0.08170625
Variance	0.0003027	0.00041677	0.00030491	0.00021254	0.00033068
GMME					
Count	4	4	4	4	16
Sum	0.3182	0.3129	0.3241	0.3963	1.3515
Average	0.07955	0.078225	0.081025	0.099075	0.08446875
Variance	0.00037055	0.00020796	0.00016044	0.00115956	0.0004566
Total					
Count	8	8	8	8	
Sum	0.6071	0.6121	0.6657	0.7739	
Average	0.0758875	0.0765125	0.0832125	0.0967375	
Variance	0.00030386	0.00027109	0.0002049	0.00059429	

ANOVA

urce of Variat	*SS*	*df*	*MS*	*F*	*P-value*	*F crit*
Sample	6.1051E-05	1	6.1051E-05	0.15577146	0.69656547	4.25967727
Columns	0.00225127	3	0.00075042	1.91469529	0.15415597	3.00878657
Interaction	0.00015171	3	5.0571E-05	0.12903188	0.94191874	3.00878657
Within	0.00940628	24	0.00039193			
Total	0.01187032	31				

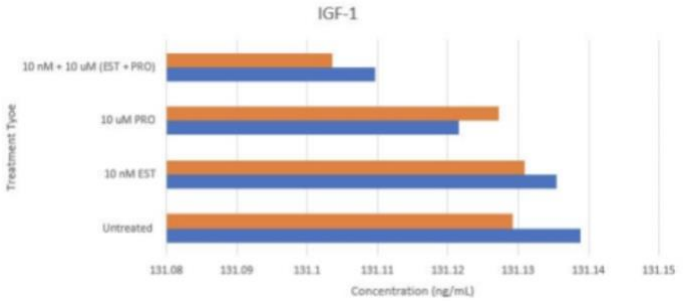

The graph shows averaged results for the IGF-1 ELISA assay. It compares L929 and GMMe cell types with treatments of estradiol, progesterone, estradiol + progesterone, along with a negative treatment with none of the hormones present. The ANOVA table depicts possible statistically significant differences between cell type and type of treatment

The IGF-1 ELISA shows a significant difference in concentration (ng/mL) between cell types across almost all of the treatments. A higher concentration is seen in the GMMe cells except for the treatment of 10 μM of progesterone, which saw the L929 cells with a higher concentration instead. In both cell types, the untreated case yields more than most of the other treated cases. The treatment that shares similar results to the untreated cases can be seen in the 10 nM estradiol case. In this study, IGF-1 is being examined in order to gauge the cell's ability to survive and proliferate. IGF was detected in each of the treatments, but the results do not exactly align with what is expected. The estradiol treatment was expected to be the case with less IGF-1 than the untreated case since an increase in the hormone also increases IGF-1 uptake. The ANOVA test performed yielded values of p that were greater than 0.05, meaning that there were no statistically significant differences present between treatment type and cell type. The error discussed earlier can be attributed to portions in the protocol where incubation was done on light-sensitive reagents. These discrepancies are likely caused by lapses in caution seen in the 2D biochemical study methods.

Examining the results of microscopy and different assays in 2D yields a lot of valuable information about the different cell types being studied. Looking at the shape of each cell with various stains allowed for a deeper understanding of their morphology and how that relates to their function within the body. In understanding endometrium cancer, observing how GMMe cells have the possibility to clump together due to their shape models successfully models tumor behavior. In addition, performing an IGF-1 ELISA allowed for the observation of normal IGF-1 levels in each cell type under different conditions. Establishing a foundation in how the different cell types respond to hormones can help model normal IGF-1 levels in order to compare to other levels in other studies that may be indicative of cancer. The presto blue assay was performed in order to observe how cell viability would be affected by hormonal treatments, and can give information on how the cell types will ultimately respond to therapies developed for the treatment of cancer. Overall, there were observations made during 2D study that will facilitate the creation of an endometrial model as it relates to cancer.

Figure 6: Average Presto Blue Results and ANOVA

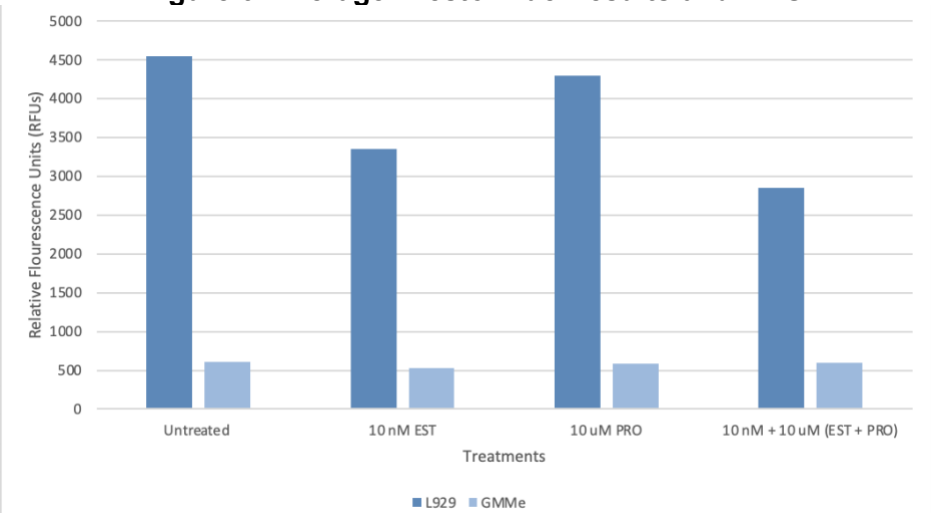

The graph displays the averaged results for the Presto Blue assay. It compares the responses of two different cell types: GMMe (shown in the light blue bars) and L929 (shown in the dark blue bars). Each cell type was subjected to four different treatments: a negative control (untreated), 10 nM of estradiol (EST), 10 uM of progesterone (PRO), and a combined treatment of estradiol and progesterone. The combined treatment caused a decrease in proliferation in the L929 cells while the treatment of 10 nM of estradiol decreased proliferation in the GMMe cells.

Anova: Two-Factor With Replication

Presto Blue					
SUMMARY	Untreated	10 nM EST	10 uM PRO	10 nM + 10 u	Total
L929					
Count	4	4	4	4	16
Sum	18189.312	13380.044	17193.239	11417.511	60180.106
Average	4547.328	3345.011	4298.30975	2854.37775	3761.25663
Variance	635517.125	2476580.41	2176190.18	2615531.67	2087970.27
GMME					
Count	4	4	4	4	16
Sum	2418.893	2122.521	2354.183	2377.884	9273.481
Average	604.72325	530.63025	588.54575	594.471	579.592563
Variance	8273.01049	5413.86875	24559.6692	15258.2948	11589.0718
Total					
Count	8	8	8	8	
Sum	20608.205	15502.565	19547.422	13795.395	
Average	2576.02563	1937.82063	2443.42775	1724.42438	
Variance	4717090.69	3326780.12	4875278.2	2586675.28	

ANOVA

urce of Variatic	*SS*	*df*	*MS*	*F*	*P-value*	*F crit*
Sample	80983889.7	1	80983889.7	81.4182128	3.5169E-09	4.25967727
Columns	3936509.77	3	1312169.92	1.3192072	0.29126209	3.00878657
Interaction	3684907.7	3	1228302.57	1.23489005	0.31884411	3.00878657
Within	23871972.7	24	994665.528			
Total	112477280	31				

Average Presto Blue Results (RFUs)

	Untreated	10 nM EST	10 uM PRO	10 nM + 10 uM (EST + PRO)
L929	4547.328	3345.011	4298.30975	2854.37775
GMMe	604.72325	530.63025	588.54575	594.471

The Presto Blue results demonstrate a notable disparity in RFU magnitude between the two cell types across all four treatments. In both cell lines, the negative treatments exhibited the highest cell proliferation as indicated by the highest RFU value. When comparing the effects of the estradiol and progesterone treatments. The estradiol treatment resulted in greater cell proliferation than in the progesterone treatment, however, the treatment involving both hormones resulted in the least proliferation in all the treatments. The ANOVA test performed on the data yielded a p-value greater than 0.05, indicating that there were no statistically significant differences observed among the treatments and the cell types. Despite the lack of statistical significance, it is important to note the qualitative differences observed in the Presto Blue results. The difference in the proliferation between the two cell types is significant where the L929 cell displayed a higher growth rate compared to GMMe cells, which can be attributed to the role L929 cells play in homeostasis and repair. Since GMMe cells are epithelial cells, they are expected to proliferate at a lower rate than L929 cells due to their primary function of lining and protecting the endometrium.

The results obtained from the 3D cell culture differ from those obtained from the 2D cell culture. In the 3D cell culture, the RFU observed of the L929 cells were significantly higher across all treatments compared to the values observed in the 2D cell culture graph. This outcome can be expected since the cells were grown on a larger surface area, causing the RFU values to increase accordingly. However, it is noted that the scaffolds without any treatment displayed the highest RFU values in the 3D culture, while in the 2D culture, the treatment with 10 uM of progesterone yielded the highest RFU. When comparing the GMMe results, it is evident that the RFU values in the 3D cell culture were significantly lower than those in the 2D cell culture. Additionally, unlike the 2D cell culture results where the RFU values for both cell types fell within a specific range, the 3D cell culture exhibited a wider range of values, with varying heights of RFU peaks.

Figure 7: Average LDH Results and ANOVA

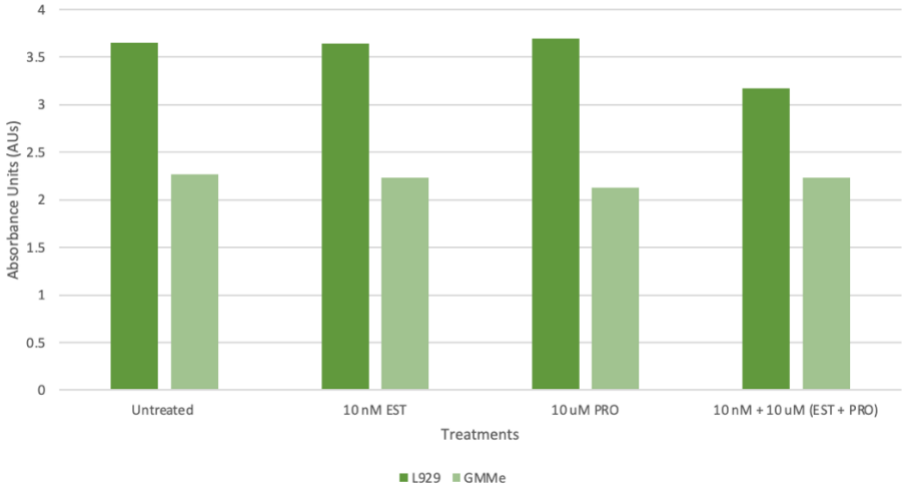

Anova: Two-Factor With Replication

LDH					
SUMMARY	Untreated	10 nM EST	10 uM PRO	10 nM + 10 u	Total
L929					
Count	4	4	4	4	16
Sum	14.6159	14.5557	14.7852	12.6759	56.6327
Average	3.653975	3.638925	3.6963	3.168975	3.53954375
Variance	0.00368273	0.01274852	0.00672145	0.92032275	0.23799239
GMME					
Count	4	4	4	4	16
Sum	9.0637	8.941	8.4995	8.916	35.4202
Average	2.265925	2.23525	2.124875	2.229	2.2137625
Variance	0.34720684	0.84687474	0.43509042	0.5291037	0.43467269
Total					
Count	8	8	8	8	
Sum	23.6796	23.4967	23.2847	21.5919	
Average	2.95995	2.9370875	2.9105875	2.6989875	
Variance	0.70086205	0.93135383	0.8948841	0.87362648	

ANOVA

ırce of Variat	*SS*	*df*	*MS*	*F*	*P-value*	*F crit*
Sample	14.0615674	1	14.0615674	36.2674288	3.226E-06	4.25967727
Columns	0.34645839	3	0.11548613	0.29786047	0.82657162	3.00878657
Interaction	0.4382643	3	0.1460881	0.3767887	0.77053971	3.00878657
Within	9.30525347	24	0.38771889			
Total	24.1515435	31				

	Average LDH Results (AUs)			
	Untreated	10 nM EST	10 uM PRO	10 nM + 10 uM (EST + PRO)
L929	3.653975	3.638925	3.6963	3.168975
GMMe	2.265925	2.23525	2.124875	2.229

The graph displays the averaged results for the LDH assay. It compares the responses of two different cell types: GMMe (shown in the light green bars) and L929 (shown in the dark green bars). Each cell type was subjected to four different treatments: a negative control (untreated), 10 nM of estradiol (EST), 10 uM of progesterone (PRO), and a combined treatment of estradiol and progesterone. The combined treatment caused a decrease in proliferation in the L929 cells while the treatment of 10 nM of estradiol decreased proliferation in the GMMe cells.

Upon analyzing the LDH results, a significant difference in absorbance units (AU) between the two cell types across all four treatments was observed. In the L929 cells, the AU values were approximately the same for the negative treatment, estradiol, and progesterone. However, the treatment involving both estradiol and progesterone exhibited lower AU values. Similarly, GMMe cells displayed a similar pattern, with comparable AU values for the negative treatment, estradiol, and the combination treatment. The progesterone resulted in the highest AU values for L929 cells, while the negative treatment yielded the highest AU values for GMMe cells.

An ANOVA test was conducted on the LDH results, demonstrating a p-value greater than 0.05 which indicates there is no statistically significant differences amount the treatments and the cell types. However, despite the lack of statistical significance, there are a few differences that reveal trends in the data. The higher AU values indicate greater cellular proliferation, reflecting increased glycolysis. Accordingly, L929 cells exhibited higher rates of cellular proliferation compared to GMMe cells. This enhanced proliferation of L929 cells can be attributed to their innate physiological properties, as they play a role in thickening the endometrium and forming the epithelial lining. Since LDH plays a vital role in glycolysis, the higher the LDH levels the higher the glycolysis activity which is a result from increased cellular proliferation and energy production.

One possible explanation for the higher AU values in L929 cells is that LDH is naturally elevated in these cells which would result in increased glycolysis. This could account for the significantly higher AU values in the L929 cells than in the GMMe cells. Additionally, considering the potential influence of human error on the differences in results could explain this change in the data. For example, insufficient cell seeding on the scaffolds during experiential set up may explain the lower AU results in the GMMe cells, although it does not account for the disparities between the two cell types. The lower AU values in GMMe cells could also be influenced by the cell viability of the scaffold, where the GMMe cells seeded may not have survived as well as L929 cells.

Conclusion and Future Work

In this study, we employed GMMe and L929 cells to investigate the effects of four different treatments: 10 nM of estradiol, 10 uM of progesterone, no treatment (control), and a combined treatment with both hormones. The objective was to assess the cellular proliferation and biochemical activity, to understand their functions within the endometrium and potential applications in endometrial cancer research Additionally, we explored the differences between 2D and 3D cell culture environments to gain insight of culture conditions and cellular behavior. The data provided insight into how GMMe and L929 cells function within the endometrium. L929 cells, known for their role in being regenerated each cycle when the endometrium is built up and shed. This suggests that L929 cells play a crucial role in growth and maintenance of endometrial tissue due to their ability to proliferate at a higher rate demonstrating their involvement in the thickening of the endometrium and facilitating tissue repair. On the other hand, GMMe cells are epithelial cells that form the protective lining of the endometrium. The lower rate s of proliferation observed in GMMe reflect their function in creating a stable and protective layer in the endometrium. These cells contribute to their barrier function of the endometrium, preventing the invasion of pathogens and providing a protective layer for the inner tissues.

Endometrial cancer is a complex disease characterized by abnormal cell growth in the endometrium. By examining the distinct behaviors of GMMe and L929 cells, research can gain insight into the mechanism underlying cancer development and progression. Higher rates of proliferation may be associated with their potential involvement in cancerous growth and formation of tumor masses. By understanding the specific factors that drive proliferation of L929 cells could provide valuable information for targeted therapeutic techniques to inhibit tumor growth. Also, differences in LDH activity and glycolytic metabolism between the two cell types could have applications in metabolic alterations associated with cancer. Since altered metabolic activity is pivotal in cancer, understanding how these changes manifest in L929 and GMMe cells is crucial to find the link between metabolism and cancer.[11]

Further exploration is needed to unravel the specific molecular mechanism underlying the differential behaviors and metabolic activities of GMMe and L929 cells within the endometrium. Investigating the genetic and epigenetic factors that contribute to these differences could provide insight into regulatory pathways in function and targets for therapies. In its context with cancer, exploring the influence of hormones and other signaling molecules on the behavior of these cells could provide insight on endocrine disruptions may contribute to cancer development. Moreover, investigating the differences between 2D and 3D cell culture environments is an important area to see the impact of scaffold composition, mechanical forces, and cell-cell interaction to mimic the *in vivo* conditions of the endometrium. Understanding how these cells interact in a 3D culture environment could have implications for tissue engineering approaches or drug screening assays that can increase patient prognosis and outcomes in cancer.[12]

References

1 Borden, L. E. *et al.* Endometrial Cancer Characteristics and Risk of Recurrence. *Am J Clin Pathol* **157**, 90-97 (2022). https://doi.org:10.1093/ajcp/aqab100

2 Zhang, X. *et al.* Single-cell transcriptome analysis uncovers the molecular and cellular characteristics of thin endometrium. *FASEB J* **36**, e22193 (2022). https://doi.org:10.1096/fj.202101579R

3 De Clercq, K. *et al.* The functional expression of transient receptor potential channels in the mouse endometrium. *Hum Reprod* **32**, 615-630 (2017). https://doi.org:10.1093/humrep/dew344

4 Yamagata, Y. *et al.* DNA methyltransferase expression in the human endometrium: down-regulation by progesterone and estrogen. *Hum Reprod* **24**, 1126-1132 (2009). https://doi.org:10.1093/humrep/dep015

5 Staff, Y. M. *Endometrial Hyperplasia*, <https://www.yalemedicine.org/conditions/endometrial-hyperplasia#:~:text=Endometrial%20hyperplasia%20is%20a%20precancerous,due%20to%20the%20excess%20bleeding.> (2023).

6 O'Brien, F. J. Biomaterials & Scaffolds for Tissue Engineering *Materials Today* **14**, 88 - 95 (2011). https://doi.org:https://doi.org/10.1016/S1369-7021(11)70058-X

7 Place, L. W. *BME 34 Lab 3 3D Cell Culture Scaffolds Slides*, <https://canvas.tufts.edu/courses/46825/files/folder/3D%20Cell%20Culture%20Scaffolds?preview=5870284> (2023).

8 Place, L. W. *BME 34 Lab 3 3D Cell Culture Biochemical Slides*, <https://canvas.tufts.edu/courses/46825/files/folder/Summary?preview=5870292> (2023).

9 Hayes, A. *Two-Way ANOVA: What It Is, What It Tells You, vs. One-Way ANOVA*, <https://www.investopedia.com/terms/t/two-way-anova.asp#:~:text=A%20two%2Dway%20ANOVA%20test,variables%20on%20a%20dependent%20variable.> (2022).

10 Place, L. W. *Turkey General Information* <https://canvas.tufts.edu/courses/46825/files/folder/Lab%20Report?preview=5986070> (2023).

11 Rawlings, T. M., Makwana, K., Tryfonos, M. & Lucas, E. S. Organiods to Model the Endometrium: Implantation and Beyond *Reproduction and Fertility* **2** (2021). https://doi.org:https://doi.org/10.1530/RAF-21-0023

12 Salinas-Vera, Y. M., Valdés, J., Pérez-Navarro, Y. & Mandujano-Lazaro, G. Three-Dimensional 3D Culture Models in Gynecological and Breat Cancer Research *Frontiers in Oncology* **12** (2022). https://doi.org:https://doi.org/10.3389/fonc.2022.826113